De Novo Discovery of Serotonin *N*-Acetyltransferase Inhibitors

Lawrence M. Szewczuk,[†,#] S. Adrian Saldanha,[‡,#] Surajit Ganguly,[§] Erin M. Bowers,[†] Margarita Javoroncov,[†] Balasubramanyam Karanam,[†] Jeffrey C. Culhane,[†] Marc A. Holbert,[†] David C. Klein,[§] Ruben Abagyan,*[,‡] and Philip A. Cole*[,†]

Department of Pharmacology and Molecular Sciences, Johns Hopkins School of Medicine, Baltimore, Maryland 21205, Department of Molecular Biology, The Scripps Research Institute, La Jolla, California 92037, and Section on Neuroendocrinology, National Institute of Child Health and Human Development, National Institutes of Health, Bethesda, Maryland 20892

Received June 5, 2007

Serotonin *N*-acetyltransferase (arylalkylamine *N*-acetyltransferase, AANAT) is a member of the GCN5 *N*-acetyltransferase (GNAT) superfamily and catalyzes the penultimate step in the biosynthesis of melatonin; a large daily rhythm in AANAT activity drives the daily rhythm in circulating melatonin. We have used a structure-based computational approach to identify the first druglike and selective inhibitors of AANAT. Approximately 1.2 million compounds were virtually screened by 3D high-throughput docking into the active site of X-ray structures for AANAT, and in total 241 compounds were tested as inhibitors. One compound class, containing a rhodanine scaffold, exhibited low micromolar competitive inhibition against acetyl-CoA (AcCoA) and proved to be effective in blocking melatonin production in pineal cells. Compounds from this class are predicted to bind as bisubstrate inhibitors through interactions with the AcCoA and serotonin binding sites. Overall, this study demonstrates the feasibility of using virtual screening to identify small molecules that are selective inhibitors of AANAT.

Introduction

Melatonin is produced in the pineal gland on a circadian schedule and is involved in the regulation of the biological clock in vertebrate organisms.[1,2] Circulating levels of melatonin rise and fall on a daily basis under the control of an endogenous circadian clock located in the suprachiasmatic nucleus. Light entrains the clock to a diurnal cycle, thus gating stimulation of the pineal gland. The biosynthesis of melatonin in the pineal gland involves the conversion of 5-hydroxytryptamine (serotonin) to 5-hydroxy-*N*-acetyltryptamine (*N*-acetylserotonin), catalyzed by serotonin *N*-acetyltransferase (arylalkylamine *N*-acetyltransferase, AANAT[a]). This is followed by O-methylation to 5-methoxy-*N*-acetyltryptamine (melatonin), which is catalyzed by 5-hydroxyindole *O*-methyltransferase (HIOMT). The rhythmic production of melatonin is controlled by large changes in the activity of AANAT. In contrast, HIOMT is constitutively active and does not regulate melatonin rhythm.[3] Efforts to understand the function of melatonin and to explore its modulation therapeutically have led investigators to develop inhibitors of AANAT. Such inhibitors have the potential to be useful in the treatment of a variety of sleep and mood disorders.[4]

Two strategies to identify AANAT inhibitors have been reported previously. One approach involved high-throughput screening, which resulted in moderately potent in vitro peptide-based inhibitors of AANAT;[4f] their utility remains to be established. A second approach, which is based on the enzyme mechanism of AANAT, focused on the development of bisubstrate inhibitors, a strategy that has been used successfully to develop inhibitors of other members of the superfamily to which AANAT belongs.[5,6] In the case of AANAT, a bisubstrate inhibitor has been developed that mimics the transient coenzyme A−*S*-acetyltryptamine (CoA−*S*-acetyltryptamine) complex that is thought to form during acetyl transfer (Figure 1). This compound is highly potent and selective for AANAT ($K_i = 90$ nM).[4i] Unfortunately, this compound exhibits no in vivo activity because its multiple phosphate groups confer poor cell permeability and unfavorable pharmacological properties.[4j] To overcome this limitation, several prodrug approaches have been devised in attempts to generate bisubstrate inhibitors in vivo within the cytoplasm.[4,7] However, because of various technical limitations, these methods have met with mixed results.[4,7]

In the study presented here, a computational approach to the identification of AANAT inhibitors has been used, one that employs virtual screening (VS) to identify candidate inhibitors with properties similar to those of known drugs (druglike).[8] This approach exploits the reported structures of AANAT in complex with bisubstrate and other coenzyme A (CoA) analogues.[9]

Achieving Selectivity over Homologous GNAT Proteins

AANAT belongs to the GCN5 *N*-acetyltransferase (GNAT) family of proteins, which share a conserved structural domain.[6a] This domain originally evolved to bind CoA through conserved backbone interactions and to facilitate acetyl transfer to a substrate. The CoA binding site is composed of two binding elements. The first is the backbone amides of a loop, known as the P-loop, which interact with the pyrophosphate oxygen atoms of CoA. The second site is a V-shaped cavity created between two parallel strands of a β-sheet. The exposed amide backbone within this cavity coordinates to the β-alanylpantetheine backbone of CoA. Interestingly, the adenine moiety of the cofactor is solvent-exposed and does not significantly contribute to binding with GNATs.[6,9,10]

This CoA binding site exhibits several positive attributes for binding druglike small molecules. First, in contrast to many

* To whom correspondence should be addressed. For R.A.: phone, 858-784-1000; fax, 858-784-8299; e-mail, abagyan@scripps.edu. For P.A.C.: phone, 410-614-8849; fax, 410-614-7717; e-mail, pcole@jhmi.edu.
† Johns Hopkins School of Medicine.
# These authors contributed equally.
‡ The Scripps Research Institute.
§ National Institute of Child Health and Human Development.

[a] Abbreviations: AANAT, serotonin *N*-acetyltransferase; GNAT, GCN5 *N*-acetyltransferase; CoA, coenzyme A; AcCoA, acetyl−coenzyme A; VS, virtual screening; HIOMT, 5-hydroxyindole *O*-methyltransferase; oAANAT, ovine serotonin *N*-acetyltransferase; αKD, α-ketoglutarate dehydrogenase; $TrpNH_2$, tryptamine; PCAF HAT, P300/CBP associated factor histone acetyltransferase; TPP, thiamine pyrophosphate; EPL, expressed protein ligation; EtOAc, ethyl acetate; NE, norepinephrine; H3−20, histone H3 residues 1−20; ICM, internal coordinate mechanics.

10.1021/jm0706463 CCC: $37.00
Published on Web 10/09/2007

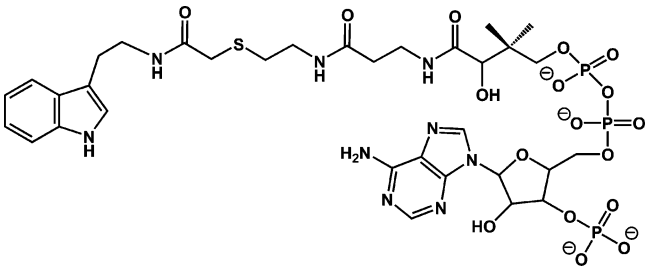

Figure 1. Structure of the bisubstrate inhibitor CoA−*S*-acetyltryptamine.

nucleotide dependent proteins, a small-molecule ligand need not mimic adenine to bind to the cofactor site. Therefore, there is less risk of nonselective binding to the multitude of nucleotide binding proteins. Second, the conserved backbone interactions may be exploited for high-affinity binding, utilizing a wide range of druglike moieties such as carboxylate, amide, or sulfonamide groups. Third, the V-shaped cavity is buried and thus provides a hydrophobic environment that is conducive to binding small druglike molecules.

Whereas the CoA binding sites of GNAT superfamily members are similar, distinct structural differences exist in the substrate binding sites, since these regions have evolved to bind a broad range of acetyl-group acceptors, including proteins and small-molecule substrates. A small-molecule candidate inhibitor that binds here would impart selectivity, but as is often the case, the cofactor binding site may enhance affinity. Thus, to gain selectivity over other homologous GNAT proteins that bind AcCoA, it is desirable for a potent and selective inhibitor of AANAT to span both sites. To this end, we describe in this report the successful use of VS to facilitate the discovery of novel inhibitors of AANAT.

Results and Discussion

Computational Analysis. In Silico Screening for AANAT Inhibitors. Docking and screening procedures, referred to as VS, can select small sets of likely lead drug candidates from large libraries of commercially or synthetically available compounds.[11] In the first stage, a nonredundant druglike commercial database of 1.2 million fully flexible ligands was docked into a grid representation of AANAT. The docking pose was then scored to maximize the discrepancy between binders and nonbinders and to rank the interaction of the compound with the receptor. This score takes into account the ligand−receptor interaction energy, conformational strain energy of the ligand, conformational entropy loss, and desolvation effects.[11c] Computational analysis (see Materials and Methods) on the top-scoring compounds resulted in the retention of a few thousand compounds. Given the expense of purchasing a few compounds from each vendor, for this proof-of-concept work we decided to limit the number of purchased compounds to those available from the Sigma-Aldrich library of rare chemicals (based on the price competitiveness of this vendor) and from the NCI repository (for which compounds are free), with a combined total of 234 501 compounds. Finally, selection based on visual inspection of the predicted docking pose resulted in 188 compounds being chosen for biological testing.

In Vitro Testing. Primary and Secondary Screens. The 188-compound subset nominated by VS was tested for its ability to inhibit ovine AANAT (oAANAT). In the primary screen, compounds that showed greater than 40% inhibition at 100 μM in an α-ketoglutarate dehydrogenase (αKD)-coupled spectrophotometric assay were assigned as potential hits.[12] A product

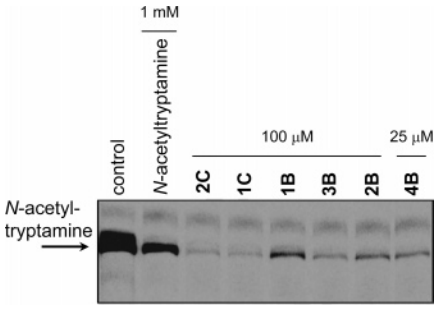

Figure 2. Verification of hits via direct [^{14}C]acetyltransferase assay. Potential hits from the primary and secondary screens were confirmed in a TLC-based assay that directly measures acetylation of $TrpNH_2$ by transfer of the [^{14}C]acetyl group from AcCoA. The 10 min reactions were carried out in 0.1 M ammonium acetate (pH 6.8), and the mixture contained 0.1 mM $TrpNH_2$, 0.1 mM [^{14}C]AcCoA. The reactions were initiated with 3.5 nM oAANAT. [^{14}C]product (*N*-acetyltryptamine) was extracted with EtOAc, resolved via TLC, and quantified by PhosphorImager analysis. The product inhibitor *N*-acetyltryptamine (1 mM) was used as a positive control.

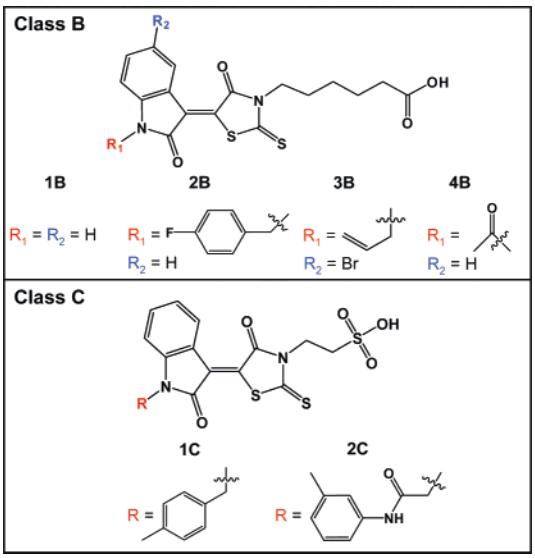

Figure 3. Structures of verified AANAT inhibitors identified by VS.

inhibitor, *N*-acetyltryptamine, was used as a positive control and exhibited an IC_{50} of 402 μM, which is consistent with the published value (Table 1).[5] The primary screen resulted in the identification of 23 potential hits. An iterative approach was taken to identify false positives. This approach included doubling the amount of αKD (to identify inhibitors that act on the coupling enzyme), rescreening in the presence of 0.01% Triton X-100 (to identify inhibitors that work by nonspecific mechanisms, such as aggregation),[13] structural validation by electrospray mass spectrometry (ESI-MS) and ^{1}H NMR, and finally, confirmation of inhibitor activity in a direct radioactive acetyltransferase assay (Figure 2).[14] Of the 23 potential hits from the primary screen, the following 5 compounds were confirmed AANAT inhibitors (Table 1, Figure 2): **1B** (L332631), **2B** (R833789), **3B** (R880868), **1C** (R825190), **2C** (R824682). These compounds fell into two classes: class B (carboxylate) and class C (sulfonate) (Figure 3). For comparison, the bisubstrate inhibitor CoA−*S*-acetyltryptamine is shown in Figure 1 and the structures of the false positives are shown in Figure 4. On the basis of the structures of these hits, a second subset of 53 compounds was tested that further explored scaffolds B and C as well as close analogues of the other potential hits from the initial screen. In an attempt to identify more potent inhibitors, the secondary screen was conducted with a more stringent cutoff

Table 1. Results from Primary Screen[a]

	% inhibition at 100 μM					
compd		(double coupling enzyme)	(0.01% Triton X-100)	structural validation	% inhibition at 100 μM (radioactive verification)	IC_{50} spec (μM)
1A	ND	ND	ND	ND	74 ± 1	402 ± 22
2A	40	X (11)				
3A	74	X (18)				
4A	42	X (24)				
5A	46	X (0)				
6A	58	X (12)				
7A	50	X (23)				
7A	46	X (14)				
8A	42	37	X (18)			
9A	42	93	X (2)			
10A	57	91	X (21)			
11A	50	31	X (220			
12A	47	66	X (4)			
13A	65	60	X (28)			
14A	99	81	88	X		
15A	100	81	100	X		
16A	100	92	65	X		
17A	98	100	79	ESI-MS	X (31)	
18A	41	30	64	ESI-MS	X (13)	
1B	100	83	78	ESI-MS/^{1}H NMR	94 ± 1	52.9 ± 2.7
2B	81	74	66	ESI-MS/^{1}H NMR	98 ± 2	45.2 ± 1.8
3B	69	62	67	ESI-MS/^{1}H NMR	98 ± 1	39.9 ± 1.2
1C	84	98	54	ESI-MS/^{1}H NMR	99 ± 1	25.2 ± 1.2
2C	99	80	70	ESI-MS/^{1}H NMR	99 ± 1	15.8 ± 1.1

[a] ND = not determined. X = compound tested and failed.

Table 2. Results from Secondary Screen[a]

	% inhibition at 25 μM					
compd		(0.01% Triton X-100)	(double coupling enzyme)	structural validation	% inhibition at 25 μM (radioactive verification)	IC_{50} spec (μM)
19A	48	X (28)				
20A	39	X (0)				
21A	52	41	X (21)			
22A	43	55	X (11)			
23A	43	59	X (0)			
24A	70	61	47	ESI-MS	X (0)	
25A	52	41	56	ESI-MS	X (0)	
4B	40	55	47	ESI-MS/^{1}H NMR	98 ± 1	28.4 ± 0.1

[a] ND = not determined. X = compound tested and failed.

of 40% inhibition at 25 μM. This resulted in the identification of eight potential candidates, of which only **4B** (L332607) was verified as an AANAT inhibitor (Table 2, Figures 2 and 3). Again, the structures of the false positives are shown in Figure 4. In the primary and secondary screens, the confirmed hit rates were approximately 2.7% and 1.9%, respectively (5 of 188 and 1 of 53). This lower hit percentage most likely reflects the fact that only a subset of commercially available VS hits were chosen for biological evaluation, namely, those available from Sigma-Aldrich or the NCI repository.

SAR of Confirmed Hits. Class B compounds contained a rhodanine scaffold with two sites of substitution on the indolinone (R_1 and R_2, Figure 3). With the exception of compound **4B**, substitution at either of these positions did not significantly change the IC_{50} value (IC_{50} = 40−50 μM). With respect to compound **4B**, acetylation of the indolinone nitrogen (R_1) resulted in an approximately 2-fold decrease in IC_{50} (from 40−50 to 25 μM). Interestingly, carboxymethylation of this nitrogen (compound **22A**) eliminates inhibitory activity of the compound, suggesting that negatively charged substituents at this position are not tolerated. It is possible that acetylation at R_1 in combination with another substitution will yield even more potent class B compounds. Class C compounds contain a similar pharmacophore compared with class B compounds except that they have a shorter alkyl arm that terminates with a sulfonate instead of a carboxylate. In general, class C compounds were more potent than class B compounds; however, the presence of the sulfonate will require a prodrug strategy to improve druglikeness. With respect to this class of compounds, a larger substitution on the indolinone nitrogen (R_1) yielded a more potent compound (compare **1C** to **2C**). The possibility for expansion with respect to the rhodanine scaffold is virtually limitless and largely unexplored. One can even imagine creating hybrid classes of compounds from these two scaffolds. For example, two additional classes can be created by substituting the acid in class B with a sulfonate and substituting the sulfonate in class C with an acid.

Ex Vivo Analysis of Representative Compounds. Because one of the goals of this project was to identify cell permeable inhibitors of melatonin biosynthesis, one inhibitor from each class (**2B** and **1C**) was selected for ex vivo evaluation in a rat pinealocyte based assay.[15] Of these compounds, only **2B** was able to inhibit melatonin biosynthesis, and inhibition was reversed upon removal of the drug from the medium (Figure 5A; compare bars 3 and 5). More extensive analysis of **2B** in this assay showed that the compound inhibited melatonin biosynthesis in a dose-dependent manner, yielding an IC_{50} in the cell-based assay of ∼100 μM (Figure 5B). Furthermore, compound **2B** did not appear to be nonspecifically toxic to the

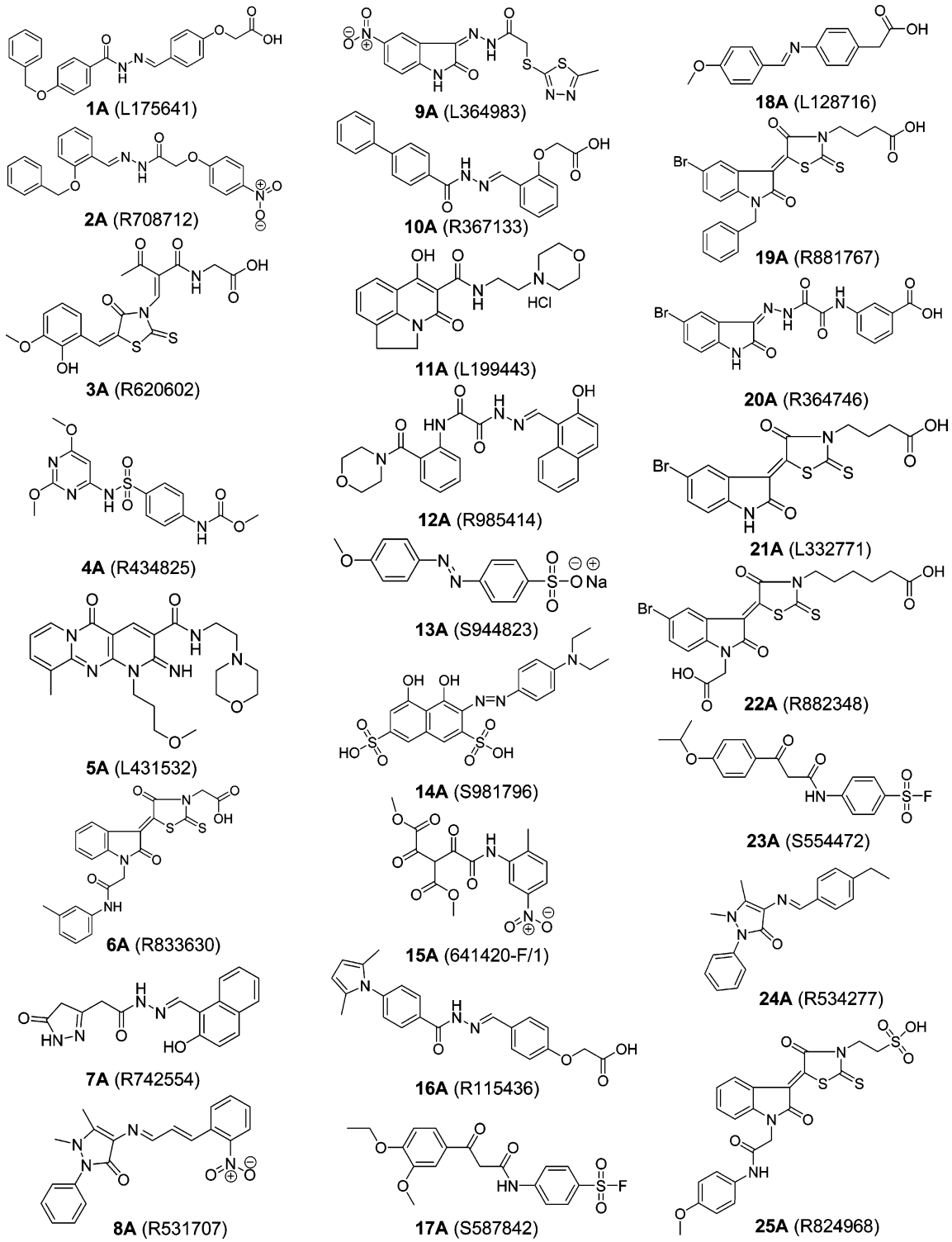

Figure 4. Structures of false positives.

cells because the amount of cellular AANAT was not altered when the concentration of **2B** was increased (Figure 5C).

Mechanistic Analysis of Class B Compounds. The mechanism of inhibition for class B compounds was probed by comparing IC_{50} values under different assay conditions. Compound **2B** was selected as the prototype for this analysis, since it showed efficacy in the cell-based assay. For this analysis, the IC_{50} was determined under three conditions using the αKD-coupled spectrophotometric assay: (i) at K_m for each substrate, (ii) at saturating tryptamine ($TrpNH_2$, $5K_m$) and K_m for AcCoA, and (iii) at saturating AcCoA ($5K_m$) and K_m for $TrpNH_2$. The following relationships were used to predict the effects of varying substrate concentrations on IC_{50} and to deduce the mechanism of inhibition:[16]

$$\text{competitive inhibition,} \quad K_i(1 + [S]/K_m) = IC_{50} \qquad (1)$$

$$\text{noncompetitive inhibition,} \quad K_i = IC_{50} \qquad (2)$$

$$\text{uncompetitive inhibition,} \quad K_i(1 + K_m/[S]) = IC_{50} \qquad (3)$$

For competitive inhibition, the IC_{50} should shift to be 3-fold less potent (to the right) when the substrate concentration is increased from K_m to $5K_m$. For noncompetitive inhibition, the

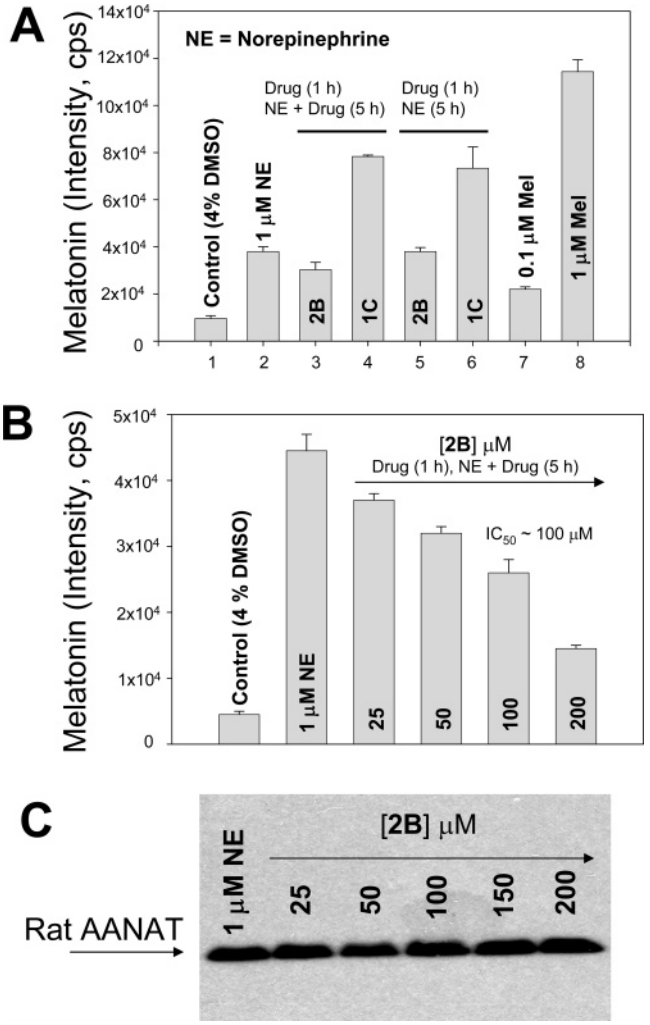

Figure 5. Cell-based screen of AANAT inhibitors. (A) Representative compounds from each class of inhibitors were evaluated for their ability to inhibit melatonin biosynthesis in rat pinealocytes. All cells received 100 μM drug for 1 h followed by either 1 μM NE + drug or 1 μM NE alone for 5 h. Secreted melatonin was quantified via liquid chromatography−quadrupole linear ion trap mass spectrometry. Melatonin values were calculated from the area of the intensity peak of the melatonin daughter ion, expressed as counts per second. (B) Compound **2B** was selected for dose response analysis in the rat pinealocyte assay. All cells received 25−200 μM **2B** for 1 h followed by 25−200 μM **2B** + NE for 5 h. Secreted melatonin was quantified as described for part A. (C) Shown are the results from Western blot analysis of resultant cell pellets from the dose response experiment with compound **2B**. Protein concentrations remain constant, indicating that the compound is not likely to be toxic to the cells over the course of the experiment.

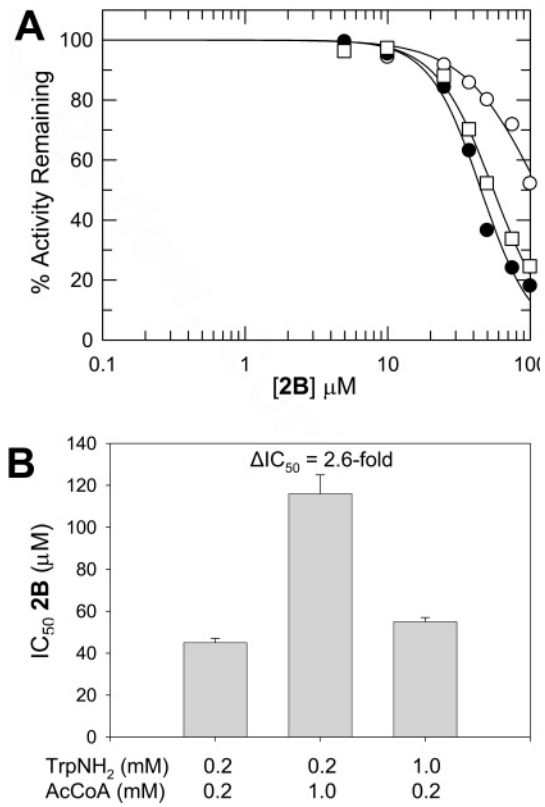

Figure 6. Mechanistic analysis of compound **2B**. IC_{50} values were used to probe the mechanism of inhibition for compound **2B**. In this analysis, the effect of raising substrate concentration (either $TrpNH_2$ or AcCoA) from K_m to $5K_m$ on IC_{50} of **2B** was determined using the αKD-coupled spectrophotometric assay. (A) IC_{50} curves under varying substrate conditions: (●) K_m $TrpNH_2$ and K_m AcCoA; (○) K_m $TrpNH_2$ and $5K_m$ AcCoA; (□) $5K_m$ $TrpNH_2$ and K_m AcCoA. (B) Replot of IC_{50} values, showing dependence on AcCoA concentration but not $TrpNH_2$ concentration.

IC_{50} should be independent of substrate concentration, and for uncompetitive inhibition the IC_{50} should shift to be 1.7-fold more potent (to the left) when the substrate concentration is increased from K_m to $5K_m$. As seen in Figure 6, IC_{50} was independent of the $TrpNH_2$ concentration and dependent on the AcCoA concentration. Furthermore, Δ IC_{50} was 2.6-fold (less potent), which is close to the predicted 3-fold change. Taken together, it is reasonable to conclude that class B compounds are competitive with respect to AcCoA and noncompetitive with respect to $TrpNH_2$. These results are consistent with class B compounds acting either as pure competitive inhibitors of AcCoA or as bisubstrate inhibitors.[17] However, in this analysis it is impossible to tell the former from the latter. It should be noted that class B compounds were predicted to be bisubstrate inhibitors of AANAT. As modeled in Figure 7A, the *p*-fluorophenyl (R_1) of compound **2B** docks in the serotonin binding site and the remainder of the hydrophobic pocket is filled by the indolinone moiety. Furthermore, the thiazolidinone carbonyl is hydrogen-bonded to the side chain of the proposed catalytic Y168. The six-carbon aliphatic linker spans the AcCoA binding site where the carboxylate is anchored by hydrogen-bonding with the backbone amide nitrogens of Q132, G136, and K135. In this manner, **2B** exploits the same backbone interactions as the β-phosphate of AcCoA.[9] As a comparison, the structure of CoA−*S*-acetyltryptamine bound to AANAT is shown in Figure 7B.

Selectivity. As the results have shown, class B compounds are cell-permeable inhibitors of melatonin biosynthesis that presumably act at the level of AANAT. Furthermore, these compounds are competitive with AcCoA. To examine the specificity of class B compounds, a prototype compound (**2B**) was evaluated for inhibition against another GNAT family member, p300/CBP-associated factor histone acetyltransferase (PCAF HAT), which binds and utilizes AcCoA in a similar manner. As demonstrated in Figure 8, compound **2B** did not inhibit PCAF at concentrations as high as 50 μM, suggesting that this scaffold imparts selectivity toward the unique substrate (i.e., serotonin) binding site of AANAT.

IC_{50} Values for Class B Compounds in the Direct Assay. As a final verification of inhibitor potency, we elected to determine the IC_{50} of **2B** and **4B** in the direct radioactive acetyltransferase assay (Figure 9).[14] The results confirmed that both compounds inhibited AANAT activity. In this assay, these inhibitors appeared to be approximately 4-fold more potent than

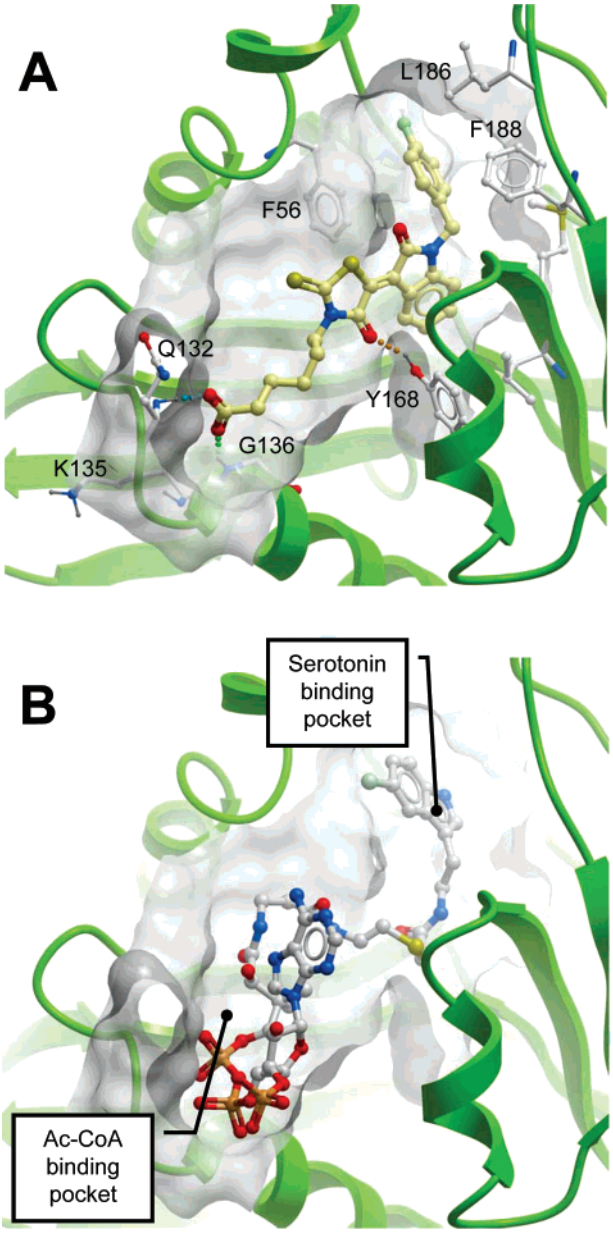

Figure 7. Proposed mode of binding of compound **2B** to oAANAT. (A) Compound **2B** docked to oAANAT. oAANAT is depicted in ribbon form and colored green. **2B** is positioned as a bisubstrate inhibitor shown as a stick model colored as follows: Carbon is yellow, oxygen is red, nitrogen is blue, and sulfur is orange. The *p*-fluorophenyl (R_1) group is docked in the serotonin binding pocket, and the remainder of this hydrophobic pocket is filled by the indolinone moiety. The thiazolidone carbonyl is hydrogen-bonded to the side chain of Y168. The six-carbon aliphatic linker spans the AcCoA binding site where the carboxylate is anchored by hydrogen bonding. Hydrogen bonds are represented by dashed gray lines. (B) Crystal structure of AANAT bound to CoA−*S*-acetyltryptamine (PDB code 1CJW). AANAT is represented as a green ribbon. CoA−*S*-acetyltryptamine is colored as follows: carbon is gray; oxygen is red; nitrogen is blue; sulfur is yellow; phosphorus is orange.

in the αKD-coupled assay. This presumably reflects the lower concentration of AcCoA in the radiochemical assay. In addition, the presence of coupling enzyme and cofactors/cosubstrates for the coupling enzyme may contribute to inhibitors appearing somewhat less potent in the spectrophotometric assay. From this analysis, the most potent class B compound was compound **4B**, which had an IC_{50} of 6.8 μM, whereas compound **2B** had an IC_{50} of 11.1 μM. This class of compounds thus represents a promising lead for further medicinal chemical development.

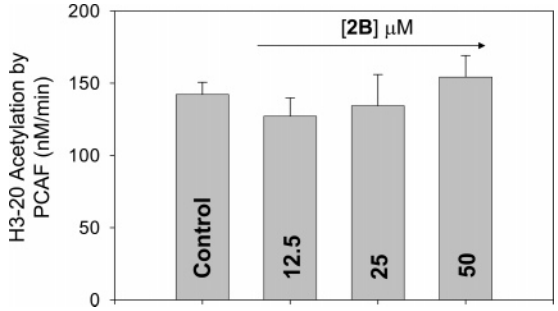

Figure 8. Evaluation of compound **2B** as a PCAF HAT inhibitor. Assays were carried out at 30 °C with reaction volumes of 30 μL that contained 10 μM substrate (H3−20) and 10 nM purified PCAF HAT domain in 50 mM Tris-HCl (pH 8.0). Reactions were initiated with 20 μM [^{14}C]AcCoA after the other components were equilibrated at 30 °C and quenched after 5 min with 6× Tris-tricine gel loading buffer. Mixtures were separated on 16% SDS Tris-tricine polyacrylamide gels and dried, and radioactivity was quantified by PhosphorImage analysis.

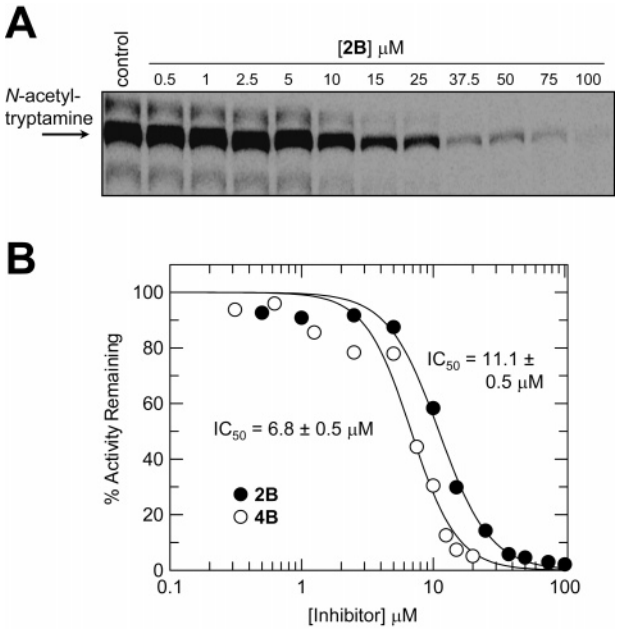

Figure 9. IC_{50} of compounds **2B** and **4B** in the direct acetyltransferase assay. In this TLC-based assay, acetylation of $TrpNH_2$ by transfer of the [^{14}C]acetyl group from AcCoA is directly monitored. The 10 min reactions were done in 0.1 M ammonium acetate (pH 6.8), and the reaction volume contained 0.1 mM $TrpNH_2$ and 0.1 mM [^{14}C]AcCoA. Reactions were initiated with 3.5 nM oAANAT. [^{14}C]product (*N*-acetyltryptamine) was extracted with EtOAc, resolved via TLC, and quantified by PhosphorImager analysis: (A) raw data from the PhosphorImage analysis showing the dose response with compound **2B**; (B) IC_{50} determination of compounds **2B** and **4B** from resultant dose response data.

Summary and Future Directions

As demonstrated with AANAT, it is possible to select, through VS, small-molecule inhibitors with selectivity and affinity. In this proof-of-concept work we selected from a subset ((1.2 million)/(230 thousand) = $^1/_5$) of total available commercial compounds and were able to identify a scaffold for lead optimization. The rhodanine nucleus identified here has also been observed to inhibit other enzymes of interest, although in these cases, it is decorated with alternative modifications.[18] In follow-up studies, we have the option to identify more inhibitor classes through selection from other vendors represented in the virtual screen or to optimize the scaffold identified in this work, as well as establish specificity versus a broader array of protein targets. The resulting AANAT inhibitors may eventually lead

to development of a drug that would be useful in circadian biology research and in the treatment of sleep and mood disorders. In the future, it would be interesting to evaluate these inhibitors against the AANAT:14-3-3ζ complex, since this complex is stable to proteolysis in vivo and ultimately responsible for elevated nighttime melatonin biosynthesis.[9e,14,19,20]

Materials and Methods

Materials. Whatman LK6D (channeled, silica gel) TLC plates and DMSO (molecular biology grade) were from Fisher Scientific. AcCoA and [^{14}C]AcCoA were from GE Healthcare. Fetal calf serum (dialyzed), bovine serum albumin (BSA), thiamine pyrophosphate (TPP), dithiothreitol (DTT), β-nicotinamide adenosine diphosphate (β-NAD), α-ketoglutaric acid, αKD (porcine heart), $TrpNH_2$, and *N*-acetyltryptamine were from Sigma-Aldrich. Papain and DNase I were from Worthington Biochemicals. Protease inhibitor cocktail was from Roche Applied Science. [^{14}C]BSA was from NEN Life Science Products. All inhibitors were purchased from either the Sigma-Aldrich rare chemical library or the NCI repository.

Molecular Modeling. All computational techniques were performed using the ICM (internal coordinate mechanics) software suite under a Linux environment. The coordinates of the protein were taken from the RCSB Protein Data Bank. Hydrogen and missing heavy atoms were added to the receptor structure followed by local minimization to resolve clashes and to correct chemistry, using a conjugate gradient algorithm and analytical derivatives in internal coordinate space.[21] Water molecules were replaced by a continuous dielectric, and the orientations of asparagine and glutamine side chains as well as the tautomeric state of histidine residues were optimized. Seven X-ray crystal structures are reported in the PDB for mammalian AANAT (six of ovine and one of human AANAT). The three liganded structures with the highest crystallographic resolution (PDB codes 1CJW, 1KUV, and 1KUX) were chosen for VS.[9a,c] All three structures contain potent bisubstrate inhibitors of AANAT. Interestingly, comparison to the unliganded (apo) structure (PDB code 1B6B)[9d] shows major ligand-induced changes in the active site. For this reason, the apo structure was not used for VS.

Compiling the Nonredundant Druglike Compound Database. Cheminformatics manipulations and analyses were performed with ICM. Ten databases, from the vendors Asinex (Russia), BioNet (England), Chembridge, Chemical Diversity, IBS (Russia), Maybridge, Sigma-Aldrich, Specs (The Netherlands), Tripos, and TimTec (Russia), in 2D SDF format and totaling 2.05 million commercially available compounds were collated. Compounds common to more than one source (redundant) or nondruglike (likely nonspecific inhibitors) were removed.[22] The following criteria were imposed to compile the nonredundant and druglike commercial database: (i) predicted solubility in water better than 1 μM; (ii) molecular weight less than 650; (iii) no atoms heavier than bromine. A library of 1.2 million compounds, stored as a single 2D SDF file, resulted from this process.

Virtual Screening. VS was performed with the ICM-Docking and ICM-VLS modules within ICM. The bisubstrate inhibitor was removed from the complexes available from the PDB, and the nonredundant druglike library was high-throughput-docked. High-throughput docking and scoring calculations were performed on a Linux cluster (up to 200-Intel Xeon processors simultaneously) at The Scripps Research Institute. An important benefit in performing VS is that a wide range of 3D descriptors is generated from the docked complex. These descriptors can then be used, in conjunction with the docking score, to improve discrimination between true binders and false positives. To implement this approach, VS results were ranked by their ICM score. The ICM scoring function includes the terms for van der Waals interactions, hydrogen bonding, electrostatics, hydrophobic interactions, desolvation, and ligand entropy loss.[23] The term weights were optimized for maximal separation of binders and nonbinders on a binding benchmark. The following three conditions were then imposed to nominate compounds for biological testing. First, a permissive cutoff score was imposed that resulted in only the top 1% of top-scoring compounds being retained. Second, the location of the ligand in the pocket was considered because the AANAT active site contains subsites for binding of cofactor (i.e., AcCoA) and substrate (i.e., serotonin). Bisubstrate ligands or ligands that occupy the serotonin binding site were preferred, since they are more likely to show high affinity and selectivity for AANAT over other members of the GNAT family. Third, the ligand should make at least one hydrogen bond with the protein. Furthermore, a conserved backbone hydrogen bond interaction with the oxygen atoms of the pyrophosphate moiety of AcCoA is characteristic of cofactor binding. Small molecules that exploit this conserved backbone interaction are preferred because they are likely to bind with higher affinity.

Protein Purification. Full length (1−207) oAANAT was prepared by expressed protein ligation (EPL) as previously described.[19] oAANAT purified via this method was >90% pure by SDS−PAGE analysis and contained a single mutation (Ala200Cys) that was necessary for the EPL reaction but did not affect enzyme activity. Protein mass was confirmed (22976 ± 60 Da) by matrix-assisted-laser-desorption-ionization (MALDI) mass spectrometry. PCAF HAT catalytic domain was purified as previously described to >90% purity by SDS−PAGE analysis.[24]

AANAT Spectrophotometric Assay. Initial screening was done by continually monitoring oAANAT acetyltransferase activity on a Beckman DU-640 spectrophotometer equipped with a thermostated cell holder (T = 25 °C), using the αKD-coupled assay as described by Kim et al.[12] This assay couples the formation of CoA to reduction of β-NAD to β-NADH (E_{340nm} = 6230 M^{-1} cm^{-1}) using αKD. Reactions (150 μL) were done in 0.1 M ammonium acetate (pH 6.8), and the reaction volume contained 50 mM NaCl, 0.2 mM β-NAD, 0.2 mM TPP, 5 mM $MgCl_2$, 1 mM DTT, 2.4 mM α-ketoglutaric acid, 0.2 mM AcCoA (K_m = 0.212 mM),[5] 0.2 mM $TrpNH_2$ (K_m = 0.147 mM),[5] 50 μg/mL BSA, and 0.1 units of αKD. Assays were initiated by addition of oAANAT (75 nM). Product formation (β-NADH) was monitored at 340 nm, and initial velocities (≤10% complete) were determined by linear regression to progress curves. Progress curves were linear to 10% complete, and initial velocities were linear with respect to oAANAT concentration to 150 nM. When inhibitors were evaluated, the DMSO concentration was held constant at 3.3%. IC_{50} values for all validated hits were determined using the following equation:

$$\%\ \text{activity remaining} = 100 \times \frac{1}{(1 + \text{I}/\text{IC}_{50})^s} \qquad (4)$$

AANAT Radioactive Assay. oAANAT acetyltransferase activity was directly monitored in a TLC-based radioactive assay that was adopted from Ganguly et al.[14] Reactions (100 μL) were done at 25 °C in 0.1 M ammonium acetate (pH 6.8), and the reaction volume contained 50 mM NaCl, 50 μg/mL BSA, 1 mM DTT, 0.1 mM TrpNH2, 0.1 mM [^{14}C]AcCoA. Reactions were initiated by addition of oAANAT (3.5 nM final). After 10 min the reactions were quenched by the addition of ethyl acetate (EtOAc, 4 volumes) and vortexing (30 s). The organic phase, which contained the reaction product (*N*-acetyltryptamine), was removed to a fresh tube, and the extraction was repeated. The pooled organic extracts were then dried in vacuo, resuspended in EtOAc (75 μL), spotted on Whatman LK6D TLC plates (25 μL), and developed in $CHCl_3$/methanol/acetic acid (90:10:1 v/v/v). Radioactivity was quantified by PhosphorImager analysis (Molecular Dynamics). Reactions did not exceed 10% completion. Product formation was linear over the course of the reaction and with respect to oAANAT concentration to 10 nM. When inhibitors were evaluated, the DMSO concentration was held constant at 3.3%. IC_{50} values of selected compounds (**2B** and **4B**) were determined in this assay using eq 4.

Pineal Cell Culture Assay. Pinealocytes were prepared from rat pineal glands as described previously.[15] Briefly, pineal glands were incubated (1 h, 37 °C) with 20 units/mL papain and 200 units/mL DNase I in Earle's balanced salt solution (EBSS). Subsequently, glands were triturated and the resulting preparation was passed through a 40 μm cell strainer (BD Falcon). The pinealocytes were

harvested, washed, and suspended in Dulbecco's modified Eagle's medium (DMEM) supplemented with 10% fetal calf serum, 2 mM glutamine, 100 units/mL penicillin, and 100 μg/mL streptomycin and incubated overnight at 37 °C (air/CO_2, 95%:5%). The following day, the cells were distributed in separate tubes (200 000 cells/250 μL) for drug treatments. Cells were first treated with drug (**2B** or **1C**) or 4% DMSO for 1 h. After 1 h, norepinephrine (NE, 1 μM) alone or in combination with drug was added to the desired tubes and incubated for an additional 5 h.

Melatonin production from the pinealocytes was estimated by a liquid chromatography−quadrupole linear ion trap mass spectrometer system (Q TRAP, Applied Biosystems).[7b] The system was connected online to an SB-C_{18} column (Zorbax, 3.5 μm, Agilent), and the data were acquired by using Analyst 1.4 software. Q TRAP was operated in positive mode with the curtain gas set to 35 (arbitrary units), and the source temperature was 350 °C. A multiple reaction monitoring (MRM) transition was selected from the list of parameters obtained after quantitative optimization of melatonin (positive mode mass 233.2). The detection method was developed by selecting parameters for a product ion (mass 174) with the highest intensity value. Optimized values of the parameters used are as follows: declustering potential, 411 V; entrance potential, 10 V; collision cell entrance potential, 20 V; collision cell exit potential, 4.0 V.

For melatonin measurement in the media (250 μL), the cells were first removed by centrifugation at 10000*g* for 10 min and the supernatants were collected and mixed with an equal volume of methanol. The supernatants were clarified by centrifugation (10000*g*, 20 min) and taken to dryness, and the residue was resuspended in 60 μL of 50% aqueous methanol. A 30 μL sample of the methanol extract of media (see above) was injected into the in-line C_{18} column using an autosampler 1100 (Agilent). The flow rate was maintained at 300 μL/min using 50% aqueous methanol as the mobile phase. The melatonin value was calculated from the area of the intensity peak (expressed as cycles per second) using the Analyst 1.4 software and a standard curve.

To detect the expression of AANAT, rat pinealocytes (that were previously treated with **2B**) were homogenized in 0.1 mM Tris-HCl, pH 7.5, containing protease inhibitor cocktail. The homogenate was subjected to a brief sonication (3 × 1 s pulses, Bronwill Scientific) and clarified by centrifugation (6000*g*, 5 min). The supernatant was boiled in Laemmli sample buffer under reducing conditions, and proteins were separated by SDS−PAGE. The proteins were then transferred onto an Immobilon-P membrane (Millipore), and AANAT was detected with a rabbit polyclonal antisera (1:10000 dilution) raised against rat the $AANAT_{25-205}$ sequence.

PCAF HAT Assay. The radioactive PCAF HAT assay was adapted from Lau et al.[24a] The reaction buffer contained 50 mM Tris-HCl (pH 8.0), 1 mM DTT, 0.1 mM EDTA, and 50 μg/mL BSA. Reactions used purified PCAF HAT enzyme at 10 nM in the presence/absence of compound **2B** (0−50 μM) in DMSO (3.3% final v/v) along with 10 μM substrate (histone H3 residues 1−20, H3−20). Assays were carried out at 30 °C with reaction volumes of 30 μL. Reactions were initiated with 20 μM [^{14}C]AcCoA after the other components were equilibrated at 30 °C and quenched after 5 min with 6× Tris-tricine gel loading buffer. Mixtures were separated on 16% SDS Tris-tricine polyacrylamide gels and dried, and radioactivity was quantified by PhosphorImager analysis (Molecular Dynamics) by comparison to known quantities of [^{14}C]BSA standard. In all cases, background acetylation (in the absence of enzyme) was subtracted from the total signal. All assays were performed in duplicate, and data agreed within 20%.

Acknowledgment. This work was supported by the NIH. R.A. is a cofounder of Molsoft and has a significant financial interest in this company. M.J. appreciates support from the MARC program, and M.A.H. was supported by the W. M. Keck Foundation.

References

(1) Arendt, J. *Melatonin and the Mammalian Pineal Gland*; Chapman and Hall: London, 1995.

(2) (a) Maestromi, G. J.; Conti, A.; Pierpaoli, W. Role of the pineal gland in immunity. III. Melatonin antagonizes the immunosuppressive effect of acute stress via an opiatergic mechanism. *Immunology* **1988**, *63*, 465−469. (b) Harlow, H. J. Influence of the pineal gland and melatonin on blood flow and evaporative water loss during heat stress in rats. *J. Pineal Res.* **1987**, *4*, 147−159. (c) Lewy, A. J.; Sack, R. L.; Miller, L. S.; Hoban, T. A. Antidepressant and circadian phase-shifting effects of light. *Science* **1987**, *235*, 352−354. (d) Iguchi, H.; Kato, K.; Ibayashi, H. Melatonin serum levels and metabolic clearance rate in patients with liver cirrhosis. *J. Clin. Endocrinol. Metab.* **1982**, *54*, 1025−1027. (e) Akerstedt, T.; Froberg, J. E.; Friberg, Y.; Wetterberg, L. Melatonin excretion, body temperature and subjective arousal during 64 hours of sleep deprivation. *Psychoneuroendocrinology* **1979**, *4*, 219−225. (f) Cohen, M.; Lippman, M.; Chabner, B. Role of pineal gland in aetiology and treatment of breast cancer. *Lancet* **1978**, *2*, 814−816.

(3) (a) Klein, D. C.; Weller, J. L. Indole metabolism in the pineal gland: a circadian rhythm in *N*-acetyltransferase. *Science* **1970**, *169*, 1093−1095. (b) Coon, S. L.; Roseboom, P. H.; Baler, R.; Weller, J. L.; Namboodiri, M. A. A.; Koonin, E. V.; Klein, D. C. Pineal serotonin *N*-acetyltransferase: expression cloning and molecular analysis. *Science* **1995**, *270*, 1681−1683. (c) Borjigin, J.; Wang, M. M.; Snyder, S. H. Diurnal variation in mRNA encoding serotonin *N*-acetyltransferase in pineal gland. *Nature* **1995**, *378*, 783−785. (d) Klein, D. C.; Roseboom, P. H.; Coon, S. L. New light is shining on the melatonin rhythm enzyme. The first post-cloning view. *Trends Endocrinol. Metab.* **1996**, *7*, 106−112. (e) Klein, D. C.; Coon, S. L.; Roseboom, P. H.; Weller, J. L.; Bernard, M.; Gastel, J. A.; Zatz, M.; Iuvone, P. M.; Rodriquez, I. R.; Begay, V.; Falcon, J.; Cahil, G. M.; Cassone, V. M.; Baler, R. The melatonin rhythm-generating enzyme: molecular regulation of serotonin *N*-acetyltransferase in the pineal gland. *Recent Prog. Horm. Res.* **1997**, *52*, 307−357. (f) Klein D.C. Arylalkylamine *N*-acetyltransferase: the Timezyme. *J. Biol. Chem.* **2007**, 282, 4233−4237.

(4) (a) Boutin, J. A.; Audinot, V.; Ferry, G.; Delagrange, P. Molecular tools to study melatonin pathways and actions. *Trends Pharmacol. Sci.* **2005**, *26*, 412−419. (b) Ferry, G.; Ubeaud, G.; Mozo, J.; Pean, C.; Hennig, P.; Rodriguez, M.; Scoul, C.; Bonnaud, A.; Nosjean, O.; Galizzi, J. P.; Delagrange, P.; Renard, P.; Volland, J. P.; Yous, S.; Lesieur, D.; Boutin, J. A. New substrate analogues of human serotonin *N*-acetyltransferase produce in situ specific and potent inhibitors. *Eur. J. Biochem.* **2004**, *271*, 418−428. (c) Zheng, W.; Cole, P. A. Novel bisubstrate analog inhibitors of serotonin *N*-acetyltransferase: the importance of being neutral. *Bioorg. Chem.* **2003**, *31*, 398−411. (d) Zheng, W.; Cole, P. A. Serotonin *N*-acetyltransferase: mechanism and inhibition. *Curr. Med. Chem.* **2002**, *9*, 1187−1199. (e) Beaurain, N.; Mesangeau, C.; Chavatte, P.; Ferry, G.; Audinot, V.; Boutin, J. A.; Delagrange, P.; Bennejean, C.; Yous, S. Design, synthesis and in vitro evaluation of novel derivatives as serotonin *N*-acetyltransferase inhibitors. *J. Enzyme Inhib. Med. Chem.* **2002**, *17*, 409−414. (f) Ferry, G.; Loynel, A.; Kucharczyk, N.; Bertin, S.; Rodriguez, M.; Delagrange, P.; Galizzi, J. P.; Jacoby, E.; Volland, J. P.; Lesieur, D.; Renard, P.; Canet, E.; Fauchere, J. L.; Boutin, J. A. Substrate specificity and inhibition studies of human serotonin *N*-acetyltransferase. *J. Biol. Chem.* **2000**, *275*, 8794−8805. (g) Kim, C. M.; Cole, P. A. Bisubstrate ketone analogues as serotonin *N*-acetyltransferase inhibitors. *J. Med. Chem.* **2001**, *44*, 2479−2485. (h) Khalil, E. M.; De Angelis, J.; Ishii, M.; Cole, P. A. Mechanism-based inhibition of the melatonin rhythm enzyme: pharmacologic exploitation of active site functional plasticity. *Proc. Natl. Acad. Sci. U.S.A.* **1999**, *96*, 12418−12423. (i) Khalil, E. M.; Cole, P. A. A potent inhibitor of the melatonin rhythm enzyme. *J. Am. Chem. Soc.* **1998**, *120*, 6195−6196. (j) Robisaw, J. D.; Neely, J. R. Coenzyme A metabolism. *Am. J. Physiol.* **1985**, *248*, E1−E9. (k) Lewczuk, B.; Zheng, W.; Prusik, M.; Cole, P. A.; Przybylska-Gornowicz, B. *N*-Bromoacetyltryptamine strongly and reversibly inhibits in vitro melatonin secretion from mammalian pinealocytes. *Neuroendocrinol. Lett.* **2005**, *26*, 581−592.

(5) De Angelis, J.; Gastel, J.; Klein, D. C.; Cole, P. A. Kinetic analysis of the catalytic mechanism of serotonin *N*-acetyltransferase (EC 2.3.1.87). *J. Biol. Chem.* **1998**, *273*, 3045−3050.

(6) (a) Vetting, M. W.; S de Carvalho, L. P.; Yu, M.; Hegde, S. S.; Magnet, S.; Roderick, S. L.; Blanchard, J. S. Structure and functions of the GNAT superfamily of acetyltransferases. *Arch. Biochem. Biophys.* **2005**, *433*, 212−226. (b) Marmorstein, R. Structure of histone acetyltransferases. *J. Mol. Biol.* **2001**, *311*, 433−444. (c) Dyda, F.; Klein, D. C.; Hickman, A. B. GCN5-related *N*-acetyltransferases: a structural overview. *Annu. Rev. Biophys. Biomol. Struct.* **2000**, *29*, 81−103. (d) Newald, A. F.; Landsman, D. GCN5-related

histone *N*-acetyltransferases belong to a diverse superfamily that includes the yeast SPT10 protein. *Trends Biochem. Sci.* **1997**, *22*, 154−155. (e) Lau, O. D.; Kundu, T. K.; Soccio, R. E.; Ait-Si-Ali, S.; Khalil, E. M.; Vassilev, A.; Wolffe, A. P.; Nakatani, Y.; Roeder, R. G.; Cole, P. A. HATs off: selective synthetic inhibitors of the histone acetyltransferases p300 and PCAF. *Mol. Cell* **2000**, *5*, 589−595.

(7) (a) Hwang, Y.; Cole, P. A. Efficient synthesis of phosphorylated prodrugs with bis(POM)-phosphoryl chloride. *Org. Lett.* **2004**, *6*, 1555−1556. (b) Hwang, Y.; Ganguly, S.; Ho, A. K.; Klein, D. C.; Cole, P. A. Enzymatic and cellular study of a serotonin *N*-acetyltransferase phosphopantetheine-based prodrug. *Bioorg. Med. Chem.* **2007**, *15*, 2147−2155.

(8) (a) Ekins, S.; Mestres, J.; Testa, B. In silico pharmacology for drug discovery: methods for virtual ligand screening and profiling. *Br. J. Pharmacol.* **2007**, 1−12. (b) Stahura, F. L.; Bajorath, J. New methodologies for ligand-based virtual screening. *Curr. Pharm. Des.* **2005**, *11*, 1189−1202.

(9) (a) Wolf, E.; De Angelis, J.; Khalil, E. M.; Cole, P. A.; Burley, S. K. X-ray crystallographic studies of serotonin *N*-acetyltransferase catalysis and inhibition. *J. Mol. Biol.* **2002**, *317*, 215−224. (b) Scheibner, K. A.; De Angelis, J.; Burley, S. K.; Cole, P. A. Investigation of the roles of catalytic residues in serotonin *N*-acetyltransferase. *J. Biol. Chem.* **2002**, *277*, 18118−18126. (c) Hickman, A. B.; Namboodiri, M. A.; Klein, D. C.; Dyda, F. The structural basis of ordered substrate binding by serotonin *N*-acetyltransferase: enzyme complex at 1.8 Å resolution with a bisubstrate analog. *Cell* **1999**, *97*, 361−369. (d) Hickman, A. B.; Klein, D. C.; Dyda, F. Melatonin biosynthesis: the structure of serotonin *N*-acetyltransferase at 2.5 Å resolution suggests a catalytic mechanism. *Mol. Cell* **1999**, *3*, 23−32. (e) Obsil, T.; Ghirlando, R.; Klein, D. C.; Ganguly, S.; Dyda, F. Crystal structure of the 14-3-3zeta:serotonin *N*-acetyltransfease complex. A role for scaffolding in enzyme regulation. *Cell* **2001**, *105*, 257−267.

(10) (a) Farazi, T. A.; Waksman, G.; Gordon, J. I. Structures of *Saccharomyces cerevisiae N*-myristoyltransferase with bound myristoylCoA and peptide provide insights about substrate recognition and catalysis. *Biochemistry* **2001**, *40*, 6335−6343. (b) Clements, A.; Rojas, J. R.; Trievel, R. C.; Wang, L.; Berger, S. L.; Marmorstein, R. Crystal structure of the histone acetyltransferase domain of the human PCAF transcriptional regulator bound to coenzyme A. *EMBO J.* **1999**, *18*, 3521−3532. (c) Vetting, M. W.; Yu, M.; Rendle, P. M.; Blanchard, J. S. The substrate-induced conformational change of mycobacterium tuberculosis mycothiol synthase. *J. Biol. Chem.* **2006**, *281*, 2795−2802.

(11) (a) Perola, E.; Walters, W. P.; Charifson, P. S. A detailed comparison of current docking and scoring methods on systems of pharmaceutical relevance. *Proteins* **2004**, *56*, 235−249. (b) Chen, H.; Lyne, P. D.; Giordanetto, F.; Lovell, T.; Li, J. On evaluating molecular-docking methods for pose prediction and enrichment factors. *J. Chem. Inf. Model.* **2006**, *46*, 401−415. (c) Totrov, M.; Abagyan, R. Protein−Ligand Docking as an Energy Optimization Problem. In *Drug−Receptor Thermodynamics: Introduction and Applications*; Raffa, R. B., Ed.; John Wiley & Sons: New York, 2001; pp 603−624.

(12) Kim, Y.; Tanner, K. G.; Denu, J. M. A continuous, nonradioactive assay for histone acetyltransferases. *Anal. Biochem.* **2000**, *280*, 308−314.

(13) (a) Di, L.; Kerns, E. H. Biological assay challenges from compound solubility: strategies for bioassay optimization. *Drug Discovery Today* **2006**, *11*, 446−451. (b) Shoichet, B. K. Screening in a spirit haunted world. *Drug Discovery Today* **2006**, *11*, 607−615.

(14) Ganguly, S.; Weller, J. L.; Ho, A.; Chemineau, P.; Malpaux, B.; Klein, D. C. Melatonin synthesis: 14-3-3-dependent activation and inhibition of arylalkylamine *N*-acetyltransferase mediated by phosphoserine-205. *Proc. Natl. Acad. Sci. U.S.A.* **2005**, *102*, 1222−1227.

(15) Schaad, N. C.; Parfitt, A.; Russell, J. T.; Schaffner, A. E.; Korf, H. W.; Klein, D. C. Single-cell $[Ca^{2+}]_i$ analysis and biochemical characterization of pinealocytes immobilized with novel attachment peptide preparation. *Brain Res.* **1993**, *614*, 251−256.

(16) Cheng, Y.-C.; Prusoff, W. H. Relationship between the inhibition constant (K_I) and the concentration of inhibitor which causes 50 per cent inhibition (I_{50}) of an enzymatic reaction. *Biochem. Pharmacol.* **1973**, *22*, 3099−3108.

(17) Yu, M.; Magalhaes, M. L. B.; Cook, P. F.; Blanchard, J. S. Bisubstrate inhibition: theory and application to *N*-acetyltransferases. *Biochemistry* **2006**, *45*, 14788−14794.

(18) Carlson, E. E.; May, J. F.; Kiessling, L. L. Chemical probes of UDP-galactopyranose mutase. *Chem. Biol.* **2006**, *13*, 825−837.

(19) Zheng, W.; Schwarzer, D.; LeBeau, A.; Weller, J. L.; Klein, D. C.; Cole, P. A. Cellular stability of serotonin *N*-acetyltransferase conferred by phosphonodifluoromethylene alanine (Pfa) substitution for Ser-205. *J. Biol. Chem.* **2005**, *280*, 10462−10467.

(20) Ganguly, S.; Gastel, J. A.; Weller, J. L.; Schwartz, C.; Jaffe, H.; Namboodiri, M. M. A.; Coon, S. L.; Hickman, A. B.; Rollag, M.; Obsil, T.; Beauverger, P.; Ferry, G.; Boutin, J. A.; Klein, D. C. Role of a pineal cAMP-operated arylalkylamine *N*-acetyltransferase/14-3-3-binding switch in melatonin synthesis. *Proc. Natl. Acad. Sci. U.S.A.* **2001**, *98*, 8083−8088.

(21) (a) Abagyan, R.; Totrov, M.; Kuznetsov, D. ICM, a new method for protein modeling and design: applications to docking and structure prediction from the distorted native conformation. *J. Comput. Chem.* **1994**, *15*, 488−506. (b) Totrov, M.; Abagyan, R. Flexible protein−ligand docking by global energy optimization in internal coordinates. *Proteins* **1997**, Suppl. 1, 215−220.

(22) (a) Lipinski, C. A.; Lombardo, F.; Dominy, B. W.; Feeney, P. J. Experimental and computational approaches to estimate solubility and permeability in drug discovery and development settings. *Adv. Drug Delivery Rev.* **2001**, *46*, 3−26. (b) Rishton, G. M. Nonlead-likeness and leadlikeness in biochemical screening. *Drug Discovery Today* **2003**, *8*, 86−96.

(23) Totrov, M.; Abagyan, R. Derivation of Sensitive Discrimination Potential for Virtual Ligand Screening. *Proceedings of the Third Annual International Conference on Computational Molecular Biology*; Lyon, France, 1999; pp 312−320.

(24) (a) Lau, O. D.; Courtney, A. D.; Vassilev, A.; Marzilli, L. A.; Cotter, R. J.; Nakatani, Y.; Cole, P. A. p300/CBP-associated factor histone acetyltranferase processing of a peptide substrate. Kinetic analysis of the catalytic mechanism. *J. Biol. Chem.* **2000**, *275*, 21953−21959. (b) Zheng, Y.; Mamdani, F.; Toptygin, D.; Brand, L.; Stivers, J. T.; Cole, P. A. Fluorescence analysis of a dynamic loop in the PCAF/GCN5 histone acetyltransferase. *Biochemistry* **2005**, *44*, 10501−10509.

JM0706463